ORIGINAL RESEARCH

D.J. Kim
T. Krings

FELLOWS' JOURNAL CLUB

Whole-Brain Perfusion CT Patterns of Brain Arteriovenous Malformations: A Pilot Study in 18 Patients

BACKGROUND AND PURPOSE: Little is known about the pathological mechanism or the anatomic and functional imaging features related to the clinical manifestations in patients with brain AVM. The purpose of this pilot study was to describe the pattern of whole-brain PCT abnormalities in brain AVMs and their potential to differentiate underlying pathomechanisms.

MATERIALS AND METHODS: Whole-brain PCT performed on a 320–detector row CT scanner was analyzed in 18 patients with untreated brain AVMs. The patterns of perfusion abnormalities on CBV, CBF, and MTT maps were analyzed and were related to clinical presentation and cerebral angiography.

RESULTS: The presenting symptoms were seizures ($n = 5$), focal neurologic deficit ($n = 5$), hemorrhage ($n = 4$), chemosis ($n = 1$), and none ($n = 3$). Three types of extranidal brain parenchymal perfusion abnormalities were noted. Decreased CBF, CBV, and MTT (pattern 1, "functional" arterial steal) were identified in 8 patients. Seizure was the most common presenting symptom in these patients ($n = 5$). Decreased CBF and CBV, and increased MTT (pattern 2, "ischemic" arterial steal) were noted in 4 patients. Focal neurologic deficit was the most common presenting symptom for these patients ($n = 3$). Increased CBV and MTT (pattern 3, venous congestion) were seen in 5 patients with presenting symptoms of neurologic deficit ($n = 2$), seizure ($n = 1$), hemorrhage ($n = 1$), and chemosis ($n = 1$). In 2 patients, pre- and posttreatment PCT was performed, which showed improvement of perfusion abnormalities.

CONCLUSIONS: Whole-brain PCT shows different patterns of perfusion abnormalities in patients with brain AVM. These perfusion patterns may discriminate the different pathologic mechanisms involved in these malformations.

ABBREVIATIONS: AVM = arteriovenous malformation; CBF = cerebral blood flow; CBV = cerebral blood volume; CTA = CT angiography; FND = focal neurologic deficit; MTT = mean transit time; PCT = perfusion CT

Brain AVM is a disease characterized by a network of abnormal direct vascular channels between the arterial feeder and the draining vein without an intervening capillary network. Schematically, 2 broad morphologic categories of arteriovenous shunts can be recognized. The nidal type is composed of a network of dysplastic plexiform vessels between the arterial feeder and the draining vein, whereas the fistulous type results from a direct connection between the artery and the vein without an intervening network. A congenital defect or a dysfunction of the embryonic capillary maturation process is expressed as the vascular malformation. It is believed that the reaction of the vascular tree to the defect and the hemodynamic alterations influence the different clinical presentations and the natural history.[1] Hemorrhage is one of the most common and well-known clinical presentations of brain AVMs and reflects the acute disturbance in the equilibrium between the malformation and the host response and is most likely caused by the high-flow angiopathy.[1] Specific angioarchitectonics of the brain AVM such as intranidal aneurysms and deep venous drainage are related to hemorrhagic presentation.[2,3] Recognition of these imaging features has significant implications in the treatment of AVMs because they provide a specific target of endovascular management.[4] On the other hand, brain AVMs may also present with symptoms such as seizures or neurologic deficits. However, little is known about the pathologic mechanisms or the anatomic and functional imaging features related to these clinical symptoms.

The purpose of this pilot study was to describe the patterns of whole-brain PCT abnormalities and differentiate the potential pathologic mechanisms of the clinical symptoms related to brain AVMs in a consecutive series of patients with these malformations.

Materials and Methods

Patients

From October 2008 to March 2010, 18 consecutive patients with brain AVMs confirmed with diagnostic angiography were prospectively recruited for the PCT study. Patients with any previous treatment of the

Received February 17, 2011; accepted after revision March 21.

From the Division of Neuroradiology (D.J.K., T.K.), Department of Medical Imaging, Toronto Western Hospital, University of Toronto, Toronto, Ontario, Canada; and Department of Radiology (D.J.K.), Yonsei University College of Medicine, Seoul, Korea.

This work was supported by a faculty research grant of Yonsei University College of Medicine for 2010 (6–2010-0150) and by a grant from the Korea Healthcare Technology R&D Project, Ministry for Health and Welfare Affairs, Republic of Korea (A085136).

Please address correspondence to Timo Krings, MD, Division of Neuroradiology, Department of Medical Imaging, Toronto Western Hospital, 399 Bathurst St, 3 McLaughling Wing, Toronto, ON, M5T 2S8, Canada; e-mail: Timo.Krings@uhn.on.ca

http://dx.doi.org/10.3174/ajnr.A2659

Table 1: Summary of cases

Case	Sex/Age (yr)	Symptom	Volume (cm^3)	Location	Drainage	PCT Abnormality Pattern (location)[a]
1	F/49	Seizure	23.0	Frontal, lt	Superficial	Pattern 1 (remote and perinidal)
2	F/40	None	2.7	Frontal, rt	Superficial	Pattern 2 (perinidal)
3	M/47	Seizure	3.8	Frontal, rt	Superficial	Pattern 1 (perinidal)
4	F/21	FND	17.2	Parietal, rt	Superficial	Patterns 1 and 2 (perinidal)
5	F/49	FND	15.3	Occipital, rt	Superficial	Pattern 3
6	F/61	none	0.4	Frontal, rt	Superficial	None
7	M/53	FND	24.7	Temporo-occipital, lt	Superficial, deep	Pattern 3
8	F/17	Hemorrhage	0.7	Temporal, rt	Superficial	None
9	M/64	Hemorrhage	2.1	Temporo-parietal, rt	Superficial	None
10	M/62	Chemosis	14.1	Frontal, rt	Superficial, deep	Pattern 3
11	F/30	None	2.4	Frontal, lt	Superficial, deep	Pattern 1 (perinidal)
12	F/28	Hemorrhage	19.1	Frontal, rt	Superficial, deep	Patterns 1 (perinidal) and 3
13	F/53	FND	10.2	Temporal, rt	Deep	Pattern 2 (remote)
14	M/39	FND	8.0	Occipital, lt	Superficial	Pattern 2 (perinidal)
15	F/42	Seizure	0.3	Parietal, lt	Superficial	Pattern 1 (perinidal)
16	M/37	Seizure	21.2	Frontal, rt	Superficial, deep	Pattern 1 (perinidal)
17	M/23	Seizure	27.4	Parietal, rt	Superficial	Patterns 1 (perinidal) and 3
18	F/39	Hemorrhage	3.1	Cerebellum, rt	Superficial	None

[a] Pattern 1 is decreased CBF, CBV, and MTT; pattern 2, decreased CBF and CBV, and increased MTT; pattern 3, increased CBV and MTT.

AVM including embolization, surgery, or radiation therapy were not included in this study. Conventional angiography, PCT maps, and clinical presentations were analyzed. Research ethics board approval was obtained for this prospective study, and subjects gave written informed consent to participate in the study.

PCT Protocol

The details for CT data acquisition are described in greater detail elsewhere.[5] Briefly, the CT data were acquired as a part of the dynamic CTA/PCT combination protocol by using the Aquilion ONE multidetector row CT scanner (Toshiba Medical Systems, Tokyo, Japan) equipped with 320 × 0.5 mm detector rows allowing coverage of a 16-cm volume during a single rotation. A test bolus scan was obtained for proper timing for maximum contrast enhancement of the internal carotid arteries before the volumetric CTA. This was followed by the dynamic acquisition sequence by using a gantry rotation speed of 1 rotation per second, a 512 × 512 matrix, and a 0.25-mm reconstruction interval. After mask image acquisition (80 kV, 300 mAs), all consecutive CTA/PCT acquisitions (80 kV, 100 mAs) allowed visualization of the passage of contrast medium through the vascular bed, thereby enabling reconstruction of both perfusion and angiographic data from the same dataset without additional contrast administration. Fifty milliliters of contrast was injected at 6 ml/s followed by 20 ml of saline. The entire scan took approximately 60 seconds. CT dose index and dose-length product were 400–450 mGy and 2230–2450 cGy/cm, respectively.

The Vitrea perfusion software (Vital Images, Minnetonka, Minnesota) was used for calculation of maps indicating the CBF, CBV, and MTT. The cerebral blood perfusion map was calculated with the so-called SVD+ deconvolution algorithm, in which SVD is the singular value decomposition and the plus stands for "delay-insensitive." This means that delayed-flow collateral circulation can be measured and displayed as a delay map.[5] The arterial input function region of interest was selected at the normal contralateral M1 segment of the internal carotid artery. The venous output function was selected at the posterior portion of the superior sagittal sinus.

Image Analysis

The CBF, CBV, and MTT maps were qualitatively analyzed by 2 neuroradiologists in consensus. The nidus and extranidal parenchyma of the whole brain were evaluated for differentiation of abnormal increase or decrease of the functional parameters (CBF, CBV, and MTT). The contralateral normal hemisphere was compared with the ipsilateral hemisphere as a reference for describing increased/decreased perfusion parameters. In general, perfusion abnormalities extending at least the width of a lobule were considered significant. The location of the perfusion abnormality was designated as perinidal (ie, immediate circumferential vicinity of the nidus) or remote.

Digital-subtraction angiograph images were analyzed for characterization of the angioarchitecture of the AVM. The images were assessed for volume of nidus, feeder, and venous drainage patterns. AVM volume was calculated on the assumption that the nidus was ellipsoid: $4/3\pi \times a/2 \times b/2 \times c/2$ (a, b, c are 3D diameters of the nidus). Nidal volume of >10 cm^3 was considered large. In addition, the arterial feeders were assessed for the presence of "sprouting" angiogenesis (defined as fine tortuous juxtanidal vessels with no early draining veins) and transdural and leptomeningeal recruitment (ie, nonsprouting angiogenesis) (defined as recruited collateral nidal feeders from adjacent pedicles of other arterial territories, "shift of the arterial watershed") on the arterial phase. The venous phase was assessed for the presence of a pseudophlebitic pattern (tortuous serpiginous engorged pial veins remote from the main draining veins)[6] and venous reflux.

Results

The characteristics of the patients are summarized in Table 1. The patients with brain AVMs consisted of 7 men and 11 women with a mean age of 41.9 years (range, 21–64 years). The mean volume of the nidus was 10.9 cm^3 (range, 0.3–27.4 cm^3). The presenting symptoms were seizures ($n = 5$), focal neurologic deficit ($n = 5$), hemorrhage ($n = 4$), chemosis ($n = 1$), and none ($n = 3$).

The nidus showed increased CBF and CBV with decreased MTT in all cases. Extranidal brain parenchymal areas of perfusion abnormalities were noted in 14 patients. All patients

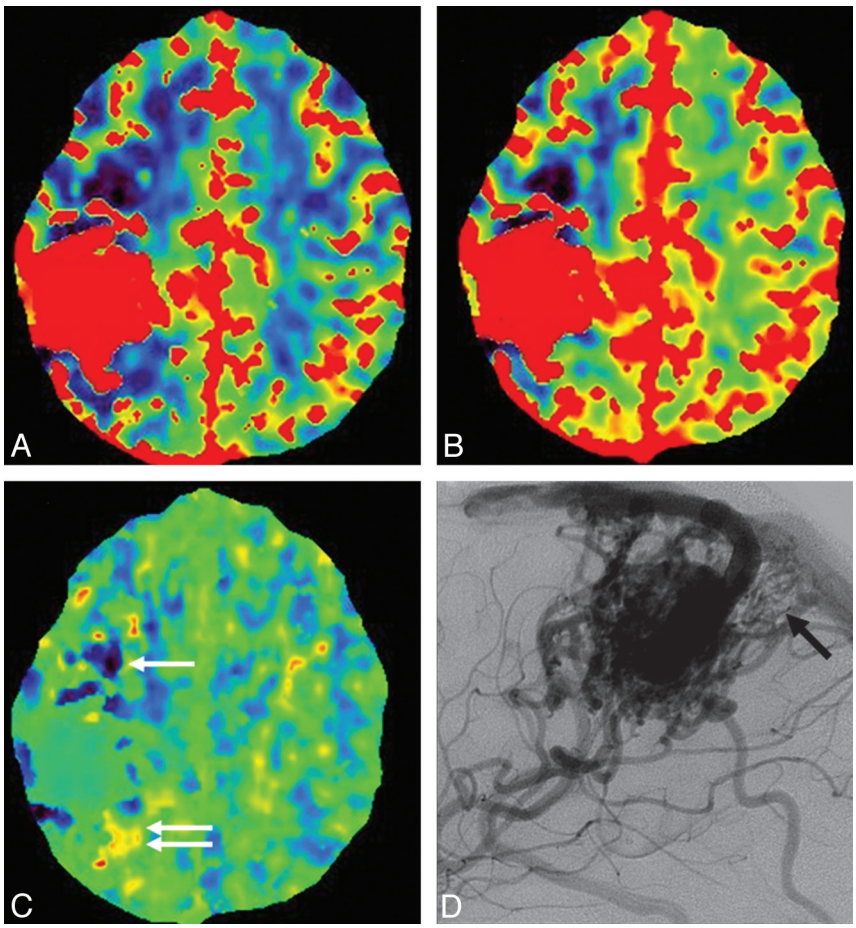

Fig 1. Case 4. *A–C*, CBF, CBV, and MTT maps. Decreased CBF and CBV are seen in the anterior and posterior perinidal areas, suggestive of arterial steal. The MTT in the anterior aspect is decreased (pattern 1, *white arrow*); however, MTT is increased in the posterior aspect (pattern 2, *white arrows*). *D*, Lateral view of conventional angiography shows small tortuous vessels posterior to the nidus, suggesting sprouting angiogenesis (*black arrow*).

with large nidal volume ($n = 9$) showed perfusion abnormalities, while 5 of 9 patients with small nidal volume (<10 cm^3) showed perfusion abnormalities. The extranidal perfusion abnormality consisted of 3 distinct patterns: extranidal areas of decreased CBF and CBV with decreased MTT (pattern 1), areas showing decrease in CBF and CBV with increased MTT (pattern 2), and areas with increased CBV and MTT (pattern 3). Two or more patterns were noted in a single patient in 3 instances (cases 4, 12, 17).

Pattern 1 was located in the perinidal area in 7 patients and in a perinidal and remote area in 1 patient. Seizure was the most common presenting symptom in the patients with this pattern ($n = 5$, Fig 1). Other symptoms included focal neurologic deficit ($n = 1$), hemorrhage ($n = 1$), and asymptomatic ($n = 1$). Pattern 2 was located in the perinidal area in 3 patients and a remote area in 1 patient. Three of the 4 patients with this pattern presented with focal neurologic deficit. Pattern 3 was seen in 5 patients (Fig 2). This pattern was only seen in patients with large nidal volume. One patient showed anterior bifrontal lobes of increased MTT compared with the posterior lobes (case 12). The presenting symptoms for these patients consisted of neurologic deficit (n = 2), seizure ($n = 1$), hemorrhage ($n = 1$), and chemosis ($n = 1$).

On the arterial phase of conventional angiography, sprouting angiogenesis ($n = 15$) was the most common finding, followed by leptomeningeal ($n = 8$) and transdural ($n = 2$) recruitment. Two or more arterial signs were observed in patients with pattern 1 (50%, 4 of 8 patients), pattern 2 (50%, 2 of 4 patients), and pattern 3 (80%, 4 of 5 patients, Table 2). On the venous phase, venous reflux was noted in 8 patients and pseudophlebitic pattern was noted in 5 patients. Two or more positive venous signs on conventional angiography were seen in 80% (4 of 5 patients) with pattern 3 compared with 13% (1 of 8 patients) in pattern 1 and none in pattern 2.

Postembolization follow-up PCT was available in 2 patients who initially presented with seizures (cases 16 and 17). Improvement of the perfusion abnormalities was noted on postembolization PCT in the 2 patients. One patient who has had seizures for 10 years showed remarkable reduction in the frequency of seizures during the 17-month follow-up (case 16). The other patient has stayed seizure-free during the 3 months of clinical follow-up (case 17, Fig 3).

Discussion

AVMs of the brain affect the intravascular pressure and may, thereby, influence the tissue perfusion in perinidal but also remote "normal" brain regions.[7] Our analysis of the whole-brain PCT maps in patients with brain AVMs revealed different distinct patterns of extranidal brain parenchymal perfusion abnormality.

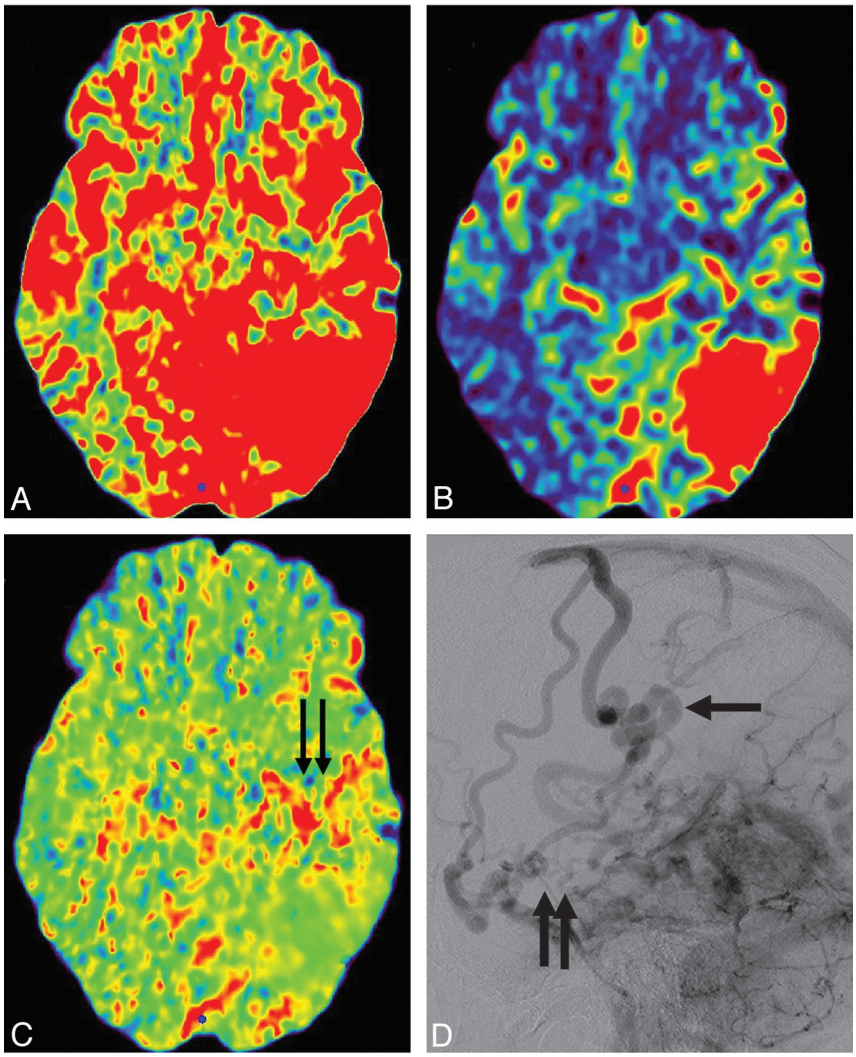

Fig 2. Case 7. *A–C*, CBF, CBV, and MTT maps. Increased CBV and MTT are seen anterior to the nidus, which is suggestive of venous congestion (pattern 3, *black arrows*). *D*, Delayed phase of lateral conventional angiography shows tortuous engorged pial veins (pseudophlebitic pattern, *black arrows*) slowly draining anteriorly in addition to the main draining vein (*arrow*).

Table 2: Catheter angiography correlated with PCT findings

	Pattern 1 (n = 8)	Pattern 2 (n = 4)	Pattern 3 (n = 5)
Arterial phase			
Neoangiogenesis (n = 15)	7 (88%)	3 (75%)	5 (100%)
Leptomeningeal recruit (n = 8)	4 (50%)	2 (50%)	4 (80%)
Transdural recruit (n = 2)	0	1 (25%)	1 (20%)
≥2 Signs	4 (50%)	2 (50%)	4 (80%)
Venous phase			
Pseudophlebitic (n = 5)	2 (25%)	0	4 (80%)
Venous reflux (n = 8)	4 (50%)	1 (25%)	5 (100%)
≥2 Signs	1 (13%)	0	4 (80%)

Arterial Steal

Decrease in CBF and CBV maps were the most common pattern of perfusion abnormality seen in 61.1% (11 of 18 patients). Such decrease of cerebral perfusion in the extranidal tissue of patients with brain AVMs has been referred to as "arterial steal."[7] "Arterial steal" is a pathologic process in which increased blood flow through a low resistance vascular bed diverts flow away from a region of the brain.[8] Distal cerebral intra-arterial pressure decreases more severely in patients with AVM compared with healthy subjects, thus exposing the areas of normal brain to relative hypotension and potential hypoxemia.[7,9] Similar patterns of perfusion abnormality have been reported in patients with ischemic stroke. In these patients, the extent of decreased CBV is strongly correlated with the final infarct size, whereas areas with decreased CBF and increased MTT are more likely to overestimate the final extent of injury.[10]

In our series, we were able to discriminate 2 different patterns of CBF and CBV decrease; MTT was decreased (pattern 1) in 1 group and increased (pattern 2) in the other group. We believe that the decrease in the MTT (pattern 1) in these patients reflects a sump effect from the vascular pedicle supplying the shunt and the adjacent normal brain tissue; thus, we hypothesize this pattern to be a functional type of steal (Fig 4). On the other hand, areas of increased MTT with decreased CBF and CBV (pattern 2) may reflect the arterial steal due to indirect collateral connection or areas remote from the nidus where the blood flow is rerouted from the normal brain toward the AVM, resulting in delayed transit time; thus, we believe this to be an ischemic type of steal. Whether the decreased CBF and CBV in our patients with the differences in MTT reflect the viability of

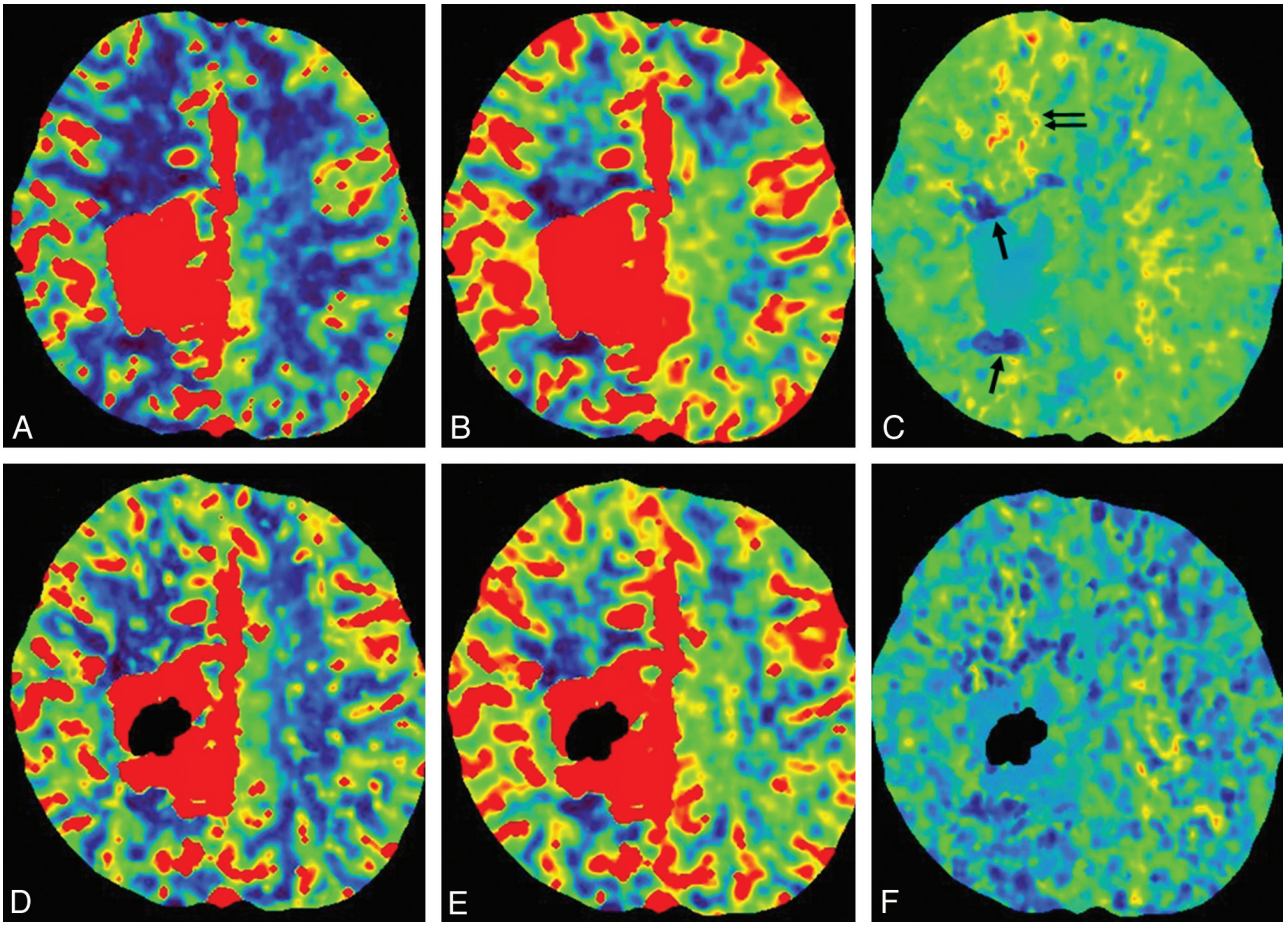

Fig 3. Case 17. *A–C*, Perinidal areas of pattern 1 are seen in anterior and posterior aspects of the nidus (*arrow*). Increased blood volume and increased transit time (pattern 3) in the remote anterior frontal lobe are suggestive of venous congestion (*arrows*). *D–F*, Postembolization CBF, CBV, and MTT maps. Glue is shown as dark signal intensity in the nidus. Improvement of pattern 3 is seen in the right frontal lobe. Residual but slight improvement of pattern 1 in the perinidal area is also suggested.

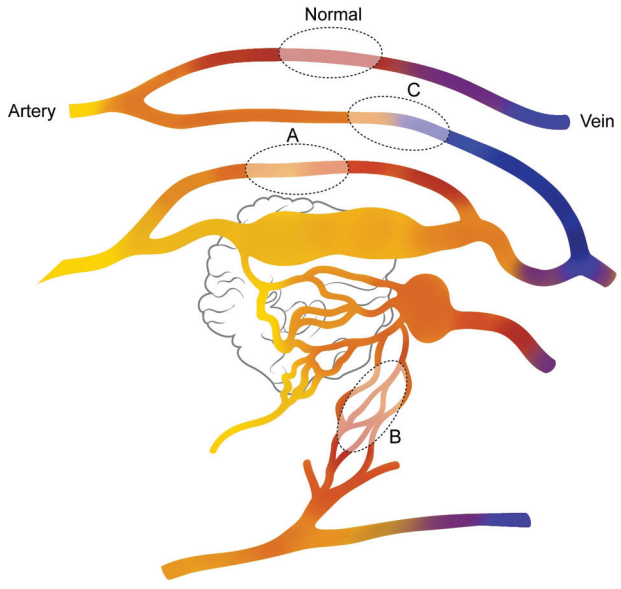

Fig 4. Schematic diagram of the PCT patterns in patients with brain AVM. Fast shunting of flow is noted in the nidus of the AVM. Blood flow in the normal brain parenchyma is seen (normal). Sump effect from the vascular pedicle supplying the shunt causes functional steal (pattern 1) in the brain adjacent to this pedicle (area A). Areas supplied by indirectly recruited collateral flow to the shunt from adjacent arteries cause ischemic steal (area B, pattern 2). High-pressure flow in the draining veins of the AVM causes venous congestion in remote parts of the brain (area C, pattern 3).

the brain tissue or reflect purely hemodynamic alterations remains to be defined.[11]

In terms of the location of such steal phenomenon, Fiehler et al[12] were able to visually identify perinidal areas of perfusion impairment in 85% of their patients by using 3D time-resolved MR angiography. They attributed the perinidal perfusion impairment to the low perfusion pressure in small arteries and arterioles. Ten of our 11 patients with decreased CBF and CBV also showed perinidal distribution of their steal.

The clinical impact related to arterial steal remains a controversy. Arterial steal is commonly considered as the explanation for the focal neurologic deficits that occur in some patients with AVMs. Decreased perfusion in patients with AVMs may cause certain neurologic deficits, and studies have shown the reversibility of the symptoms and perfusion defects after treatment.[13,14] Seizures have also been attributed to steal.[15] Hypoxemia-induced destruction of neurons transmitting or secreting γ-aminobutyric acid may lead to intracortical hyperexcitability.[16] However, some authors have ascribed the steal phenomenon to neuronal loss in chronic hypoxemic areas. In a positron-emission tomography study, the perinidal tissue with low blood flow showed decreased glucose and oxygen metabolism, suggesting neuronal loss in chronically hypoperfused areas.[17] Dilated capillaries with gliotic changes have been identified in the immediate perinidal parenchyma; thus some

of the symptoms attributed to the steal phenomenon may actually reflect symptoms related to the gliosis from chronic steal.[7,11] In our series, both focal neurologic deficit and seizure were seen with arterial steal. Pattern 1 (functional steal) was more often associated with seizures (5 of 7 cases), and pattern 2 (ischemic steal) was more often associated with focal neurologic deficits (3 of 4 cases).

Venous Congestion

Another distinct pattern of perfusion abnormality was increased CBV and MTT (pattern 3, $n = 5$). High-flow shunt in the brain (which may be associated with venous outflow restrictions) may overload the venous system and preclude normal venous drainage, causing venous congestion (Fig 2). This causes increased blood volume and delayed transit time.[18] Venous congestive encephalopathy may cause reversible focal neurologic deficit or seizures.[18] The symptoms in our series included neurologic deficit, seizure, hemorrhage, and chemosis. Chemosis was the direct manifestation of congestive reflux of the shunted flow into the superior ophthalmic vein in 1 patient (case 10).

The venous congestion seen on PCT correlated with the conventional angiography features of congestion, such as venous reflux and pseudophlebitic pattern. Eighty percent of the cases with pattern 3 (4 of 5 cases) showed ≥ 2 angiographic features of venous congestion compared with 13% (1 of 8 cases) for pattern 1 and none in pattern 2. However, no definite catheter angiographic findings were able to discriminate between patterns 1 and 2. In some cases, >1 pathologic mechanism may be present in a single patient either in the same or different areas of the brain. In our series, 3 patients showed >1 pattern of PCT abnormality. Pattern 2 coexisted with pattern 1 in 1 patient. Pattern 3 coexisted with pattern 1 in 2 patients. The locations of the PCT abnormalities in a patient were different in our patients with multiple patterns; however, it is plausible that in some patients, different pathologic mechanisms affect the same area of the brain, which may confound and mask abnormal PCT findings.

Therapeutic Implications

Identification of the pathomechanism and scrutinizing of the imaging features that are directly related to the clinical presentation could allow targeted treatment and improved clinical outcome.[4,19] For patients with hemorrhage, the primary target for embolization is the angioarchitectural weak point (eg, pseudoaneurysm).[4,20] For patients with other clinical presentations, little is known about the imaging features responsible for the symptoms or the imaging criteria for evaluation of the treatment efficacy.

The degree of arterial hypotension is related to the magnitude of flow through the fistula, thus a direct fistulous connection may be more prone to steal than a nidus type of connection.[7] High-flow fistula with venous outflow obstruction may also cause venous congestion due to venous overload along with secondary changes such as pseudophlebitic pattern and venous reflux. These features may be localized to a specific compartment of the AVM, which may be geographically targeted. In our 2 cases with pre- and postembolization PCT studies (cases 16, 17), targeted embolization of the high-flow fistulous connections resulted in the improvement of clinical symptoms and PCT abnormalities. This implies the role of PCT not only as a tool for verifying the pathologic mechanism of the AVM but also as a potential tool for assessment of the posttreatment efficacy. Nevertheless, in some cases, the accompanying pathologic changes (eg, perinidal gliosis) or a secondary cerebral focus may be the culprit of the symptoms, and in these cases, targeted embolization may not result in clinical improvement.[21] A larger scale study is necessary for further validation of these results.

Conclusions

Whole-brain PCT shows different distinct patterns of perfusion abnormalities in patients with brain AVMs. These perfusion patterns may help to discriminate the different pathologic mechanisms involved in the disease with potential therapeutic implications.

References

1. Berenstein A, Lasjaunias PL, Ter Brugge K. *Surgical Neuroangiography: Clinical and Endovascular Treatment Aspects in Adults.* 2nd ed. Berlin, Germany: Springer-Verlag; 2004:609–94
2. Mast H, Young WL, Koennecke HC, et al. **Risk of spontaneous haemorrhage after diagnosis of cerebral arteriovenous malformation.** *Lancet* 1997;350:1065–68
3. Redekop G, TerBrugge K, Montanera W, et al. **Arterial aneurysms associated with cerebral arteriovenous malformations: classification, incidence, and risk of hemorrhage.** *J Neurosurg* 1998;89:539–46
4. Meisel HJ, Mansmann U, Alvarez H, et al. **Effect of partial targeted N-butyl-cyano-acrylate embolization in brain AVM.** *Acta Neurochir (Wien)* 2002;144:879–87, discussion 888
5. Salomon EJ, Barfett J, Willems PW, et al. **Dynamic CT angiography and CT perfusion employing a 320-detector row CT: protocol and current clinical applications.** *Klin Neuroradiol* 2009;19:187–96. Epub 2009 Aug 23
6. Willinsky R, Goyal M, terBrugge K, et al. **Tortuous, engorged pial veins in intracranial dural arteriovenous fistulas: correlations with presentation, location, and MR findings in 122 patients.** *AJNR Am J Neuroradiol* 1999;20:1031–36
7. Kader A, Young WL. **The effects of intracranial arteriovenous malformations on cerebral hemodynamics.** *Neurosurg Clin N Am* 1996;7:767–81
8. Symon L. **The concept of intracerebral steal.** *Int Anesthesiol Clin* 1969;7:597–615
9. Fogarty-Mack P, Pile-Spellman J, Hacein-Bey L, et al. **The effect of arteriovenous malformations on the distribution of intracerebral arterial pressures.** *AJNR Am J Neuroradiol* 1996;17:1443–49
10. Lev MH, Nichols SJ. **Computed tomographic angiography and computed tomographic perfusion imaging of hyperacute stroke.** *Top Magn Reson Imaging* 2000;11:273–87
11. Attia W, Tada T, Hongo K, et al. **Microvascular pathological features of immediate perinidal parenchyma in cerebral arteriovenous malformations: giant bed capillaries.** *J Neurosurg* 2003;98:823–27
12. Fiehler J, Illies T, Piening M, et al. **Territorial and microvascular perfusion impairment in brain arteriovenous malformations.** *AJNR Am J Neuroradiol* 2009;30:356–61
13. Marks MP, Lane B, Steinberg G, et al. **Vascular characteristics of intracerebral arteriovenous malformations in patients with clinical steal.** *AJNR Am J Neuroradiol* 1991;12:489–96
14. Sugita M, Takahashi A, Ogawa A, et al. **Improvement of cerebral blood flow and clinical symptoms associated with embolization of a large arteriovenous malformation: case report.** *Neurosurgery* 1993;33:748–51, discussion 52
15. Weinand ME. **Vascular steal model of human temporal lobe epileptogenicity: the relationship between electrocorticographic interhemispheric propagation time and cerebral blood flow.** *Med Hypotheses* 2000;54:717–20
16. Luhmann HJ, Kral T, Heinemann U. **Influence of hypoxia on excitation and GABAergic inhibition in mature and developing rat neocortex.** *Exp Brain Res* 1993;97:209–24
17. Fink GR. **Effects of cerebral angiomas on perifocal and remote tissue: a multivariate positron emission tomography study.** *Stroke* 1992;23:1099–105
18. Lagares A, Millan JM, Ramos A, et al. **Perfusion computed tomography in a dural arteriovenous fistula presenting with focal signs: vascular congestion as a cause of reversible neurologic dysfunction.** *Neurosurgery* 2010;66:E226–27, discussion E227
19. Krings T, Hans FJ, Geibprasert S, et al. **Partial "targeted" embolisation of brain arteriovenous malformations.** *Eur Radiol* 2010;20:2723–31. Epub 2010 Jun 11
20. da Costa L, Wallace MC, Ter Brugge KG, et al. **The natural history and predictive features of hemorrhage from brain arteriovenous malformations.** *Stroke* 2009;40:100–05
21. Yeh HS, Kashiwagi S, Tew JM Jr, et al. **Surgical management of epilepsy associated with cerebral arteriovenous malformations.** *J Neurosurg* 1990;72:216–23